

Large septic pulmonary embolus complicating streptococcus mutans pulmonary valve endocarditis

Christian Andres Inchaustegui^{1*}, Kevin Yuqi Wang², Oluwadamilola Teniola², Veronica Lenge De Rosen²

1. Facultad de Medicina Alberto Hurtado, Universidad Peruana Cayetano Heredia, Lima, Peru

2. Department of Radiology, Baylor College of Medicine, Houston, Texas, USA

* **Correspondence:** Christian Andres Inchaustegui, 611 NW 159th Ave, Pembroke Pines, FL 33028, USA
(✉ christian.inchaustegui@upch.pe)

Radiology Case. 2018 Feb; 12(2):18-27 :: DOI: 10.3941/jrcr.v12i2.3240

ABSTRACT

Large septic pulmonary embolus is a rare finding in right-sided endocarditis. The entity represents a challenging diagnosis due to its variable and nonspecific clinical and radiological presentation and similarities with other conditions. We present a case of a 41 year-old woman who developed a large main pulmonary artery embolus and bilateral cavitory lung nodules in the setting of severe sepsis. Pulmonary artery exploration and clot retrieval ultimately revealed a large septic embolus from *Streptococcus mutans* native pulmonary valve endocarditis. The diagnosis of septic pulmonary emboli from right-sided endocarditis should be considered in patients with ancillary findings of septic embolic phenomenon, particularly the presence of multifocal cavitory nodules and in the setting of appropriate predisposing factors.

CASE REPORT

CASE REPORT

A 41-year-old female with a past medical history of cervical squamous cell carcinoma and pulmonary valve stenosis was admitted following a 2-week history of fever and shortness of breath. Family and social history were unremarkable. Vital signs were notable for low-grade fever and tachypnea, and physical exam was notable for a systolic ejection murmur and poor dentition. Initial laboratory workup revealed leukocytosis and acute kidney injury. She was started on intravenous fluids and antibiotics. Overnight, the patient suddenly developed worsening tachypnea and hypoxemia but remained hemodynamically stable.

Chest radiograph demonstrated findings suggestive of interstitial pulmonary edema (Fig. 1). Modified Well's score suggested a high likelihood of pulmonary embolism. Computed tomographic pulmonary angiography (CTPA) revealed a large pulmonary embolus at the main pulmonary artery bifurcation without radiological evidence of right heart strain (Fig. 2). Additionally, multiple lower lobe-predominant

peripheral nodules, some which were cavitory, were seen in random distribution throughout both lungs, concerning for septic emboli (Fig. 3).

The patient was started on an intravenous heparin drip, supplemental oxygen, and continued on intravenous antibiotics. Blood cultures returned positive for *Streptococcus mutans*. Subsequent transthoracic echocardiogram did not show vegetations on the tricuspid or pulmonary valves, but demonstrated a peak pressure gradient of 80 mmHg at the level of the pulmonary valve (Fig. 4), consistent with severe stenosis. Lower extremity duplex for deep venous thrombosis was unrevealing (Fig. 5) and troponins and serum brain natriuretic peptide were undetectable. Transesophageal echocardiogram was not attempted as the patient was thrombocytopenic and considered unstable for the procedure. The patient progressed unfavorably with further episodes of worsening tachycardia, fever and tachypnea.

Repeat CTPA 10 days following the initial scan showed interval increase in the number of lower lobe-predominant

subpleural nodules (Fig. 6) and new pleural-based consolidations (Fig. 7), thought to reflect increasing septic emboli burden. Furthermore, a new pulmonary embolus was seen in a right upper lobe segmental pulmonary artery (Fig. 8). Despite intravenous antibiotic treatment according to culture susceptibilities, the patient continued to progress unfavorably with severe sepsis and worsening renal insufficiency.

She subsequently underwent pulmonary artery exploration and embolectomy. An organized pulmonary artery thrombus measuring up to 2.5 cm in maximal diameter attached to the anterior wall of the main pulmonary artery and a 0.5 cm vegetation in the posterior pulmonary valve annulus were found. Both were excised and the pulmonary valve was reconstructed. Pathology report (Fig. 9) from the embolus revealed a thrombus with numerous bacterial microorganisms.

The patient's clinical course improved with resolution of her severe sepsis and acute kidney injury. Subsequent blood and surgical specimen cultures were negative. The patient was discharged on post-procedural day 14 with a 6-week course of intravenous antibiotics.

DISCUSSION

Etiology & Demographics:

Pulmonary valve endocarditis (PVE) comprises 2% of all endocarditis admissions [1]. Similarly, the reported frequency of septic pulmonary emboli (SPE) among all autopsy-proven pulmonary embolism cases was 2.2% in a postmortem study [2]. Right-sided infective endocarditis is cited as the most common source of SPE [3,4] with the majority of emboli arising from tricuspid valve vegetations. Other sources of SPE distinct from endocarditis include infected central lines or devices (pacemakers), deep soft tissue infections (osteomyelitis, fasciitis and cellulitis), peripheral septic thrombophlebitis (Lemierre's syndrome, septic pelvic vein thrombophlebitis) and deep abscesses [5].

The majority of cases of PVE and SPE occur in patients with congenital heart disease, intravenous drug use, alcoholism, central intravenous lines, and prosthetic valves [6,7]. Various immunodeficiency states including solid and hematological cancers, human immunodeficiency virus infection, diabetes mellitus, and organ transplantation are also important risk factors [2,5]. There is no age or gender predilection for SPE. Our patient's predisposing severe pulmonic stenosis increased her risk for endocarditis. Moreover, given non-valvular vegetations in endocarditis are usually found at the site of impact of high velocity jets [8], the high-pressure jet across the valve seen on transthoracic echocardiogram may have further predisposed to the large septic embolus ultimately seen along the anterior wall of the pulmonary artery.

The most common pathogen responsible for SPE is *Staphylococcus aureus* [9], with methicillin-resistant *Staphylococcus aureus* comprising 40% of *S. aureus* cases [5]. Other common agents include *Candida* sp., *Fusobacterium* sp.,

Klebsiella pneumoniae and *Streptococcus viridans* [9], but the relative frequency of each agent varies according to the underlying etiology leading to SPE [5]. In this patient, the primary origin of her bacteremia was probably odontogenic, as poor dentition was evident on physical exam with biochemical and imaging findings not revealing of other etiologies. *Streptococcus mutans* is a normal member of the oral flora and the main microorganism associated with dental caries. Furthermore, it is a member of the viridans streptococci group, which causes 18% of all infective endocarditis cases [10]. Overall, the combination of endodontal-peridontal disease and pulmonic valve stenosis probably significantly predisposed her to endocarditis.

Clinical & Imaging findings:

Not surprisingly, given the systemic process, the presentation of SPE is nonspecific. A systematic review of observational studies from 1978 to 2012, which included 168 cases of SPE, found that the most common clinical features were fever, dyspnea, chest pain and cough [9], which were all features in our patient.

The diagnosis of SPE is a clinical-radiological one, which is commonly based on criteria proposed by Cook et al. [11] and include: 1) focal or multifocal lung infiltrates compatible with septic embolism in the lung, 2) presence of an active extra-pulmonary source of infection as a potential embolic source, 3) exclusion of other potential explanation for lung infiltrates and 4) resolution of lung infiltrates with appropriate antibiotic therapy.

Imaging may provide more specific findings of SPE. On chest radiograph, nonspecific lower lobe infiltrates are the most common abnormality [12]. Peripheral opacities with cavitation, although highly suggestive of SPE [12], are unusual, only found on approximately 20% of chest radiographs [9,12]. On chest CT imaging, the most common finding is multiple peripheral lung nodules, occurring in 66% to 93% of affected patients in two different case series [5,9]. Nodules are soft tissue density, well- or ill-defined, and range from 0.5 cm to 3.5 cm in diameter [13]. Cavitation is reported to occur in approximately 55% to 67% of cases [5,9] and is associated with gram-positive organisms as the etiologic agent [13], as seen in our case. The lesions are bilateral and multiple in approximately 90% of patients [5,9].

A pulmonary artery branch traversing to the nodule, termed the "feeding vessel sign", is a nonspecific finding but suggests a hematogenous spread of the pulmonary nodule [14]. SPE, bland pulmonary embolism, and pulmonary metastasis can all present with nodules featuring this sign. Furthermore, an area of central consolidation with peripheral ground-glass opacity, termed the "CT halo sign", is a characteristic but nonspecific imaging finding that is reflective of surrounding hemorrhagic infarction in the context of SPE [13]. The halo is also a feature of other diseases, including hemorrhage from metastases and fungal angioinvasion seen in aspergillus, zygomycetes and candida [13]. Both the CT halo sign and feeding vessel sign are reported to occur in approximately 30% of cases, and are more frequent with gram-negative organisms [9,13]. Wedge-shaped subpleural consolidations

(commonly reflective of pulmonary infarcts) and pleural effusions are other features that occur in SPE in 17% and 30% of cases respectively [9], and may also be seen in bland pulmonary emboli [12,14].

Most emboli in SPE occlude segmental or subsegmental pulmonary arteries [12], with one study reporting involvement of the segmental pulmonary arteries in approximately 50% of cases [4]. The presence of a large septic central pulmonary embolus in the main pulmonary artery, as seen in the current case, is rare. To our knowledge, only 3 publications reporting native PVE complicated by SPE with a large filling defect on a central pulmonary artery on chest CT [1,6,15] have been published. One of the reports corresponded to candida endocarditis and the two others did not isolate an organism. Large filling defects also occur in bland pulmonary embolism, but the simultaneous presence of multiple lower lobe-predominant, randomly distributed, peripheral cavitory nodules points toward SPE [15].

The rapid development of bronchiectasis in our patient (Figure 7) is unusual. Bronchiectasis often occurs in the context of chronic inflammatory changes and it is counterintuitive to observe the development in our case in such a short time span (10 days). Bronchiectasis is a very heterogeneous condition and the end result may be due to a variety of factors [16]. Consequently, the pathophysiologic processes are difficult to delineate and this likely contributes to the approximate 50% idiopathic etiology. Nevertheless, approximately 25% are thought to be post-infectious, and cases of relatively rapid progression of bronchiectasis have been reported, albeit spanning over several months [17]. The rapid development in our patient is certainly an exception and meaningful conclusions from one case are difficult to ascertain. Nevertheless, we speculate perhaps that the substantial bacterial load and infectious burden from the large septic embolus may have somehow accelerated the development of post-infectious bronchiectasis.

Treatment & Prognosis:

Management of SPE involves treating the underlying infection with intravenous antibiotics [5]. In the case of PVE, a 6 week antibiotic regimen with *S. aureus* coverage is commonly used [18]. In certain settings, such as in our patient, procedural intervention is required to eliminate the infectious focus [5,9]. Anticoagulation for SPE, especially in the setting of right sided endocarditis is controversial, mainly due to the risk of hemorrhage from potential central nervous system (CNS) embolization [5]. Anticoagulation may diminish the risk of embolization [18] and thus its use should be individualized according to the competing risks of embolism and hemorrhage [5,18]. Our patient had a large pulmonary embolus when anticoagulation was started, and due to increasing embolic burden, respiratory decompensation, and a lack of the predisposed risk of CNS embolization in the setting of left-sided endocarditis, anticoagulation was continued. Mortality from SPE is high despite treatment, ranging from 10 to 20%, most commonly from septic shock and multi-organ failure [5,9].

Differential Diagnoses:

The differential diagnosis of SPE manifesting as multiple pulmonary nodules with cavitation on CT includes metastatic lung disease, granulomatosis with polyangiitis (GWP), necrobiotic lung nodules (NLN), chronic necrotizing aspergillosis (CNA) and pulmonary tuberculosis [19, 20].

Metastatic lung disease:

Metastatic lung disease, particularly squamous cell carcinomas, adenocarcinomas, and sarcomas can present with multiple randomly distributed cavitory nodules of varying sizes and wall thickness [19]. Moreover, metastatic malignancies can manifest as large intravascular filling defects on the central pulmonary arteries, resulting from tumor emboli after invasion of the inferior vena cava, but the neoplasms associated with this presentation (hepatoma, renal cell carcinoma and choriocarcinoma) [21] are different than the ones presenting with cavitating lung nodules (squamous carcinomas from the cervix, lung, gastrointestinal tract and breast, sarcomas and adenocarcinomas) [19,22]. From the latter group, only breast carcinoma has been reported to be a common cause of tumor emboli but in a peripheral distribution [21]. Malignant disease can be differentiated from SPE by the dynamic nature of the latter condition in which new nodules and cavitation develop over a matter of days [19]. Calcification is also a feature that can be found in metastatic sarcomas and adenocarcinomas but not in SPE [21]. A main concern in our patient was the possibility of metastatic squamous cervical cancer due to her past medical history, but the rapidly evolving course of the nodules on the 10-day repeat CTPA favored SPE.

Granulomatosis with polyangiitis:

GWP features larger nodule sizes than SPE, ranging on average from 2 to 4 cm, and may be up to 10 cm [19,20]. In comparison, SPE nodules range from 0.5 to 3.5 cm. Nodules in GWP are typically located centrally [19] and do not exceed 10 in number [20], whereas nodules in SPE tend to be peripheral and subpleural, with up to a third of cases having more than 10 nodules [5].

Necrobiotic lung nodules:

NLN consist of cavitating nodules occurring in the context of rheumatoid arthritis [19] or inflammatory bowel disease [20]. This condition features nodules that are also peripheral and subpleural, but unlike SPE the condition is frequently asymptomatic [19]. Feeding vessels and CT halo signs are also not a feature.

Chronic necrotizing aspergillosis:

CNA is an indolent and semi-invasive form of angioinvasive aspergillosis that classically presents as an apical solitary, slow-growing cavitating nodule [20], but in patients with multiple lesions, its distinction from SPE may sometimes present a challenge. Both exhibit peripheral or subpleural lesions, CT halo and feeding vessel signs [19], and present with fever, dyspnea, cough or hemoptysis [23]. Unlike invasive aspergillosis, CNA presents in patients with a milder immunocompromised state (e.g. steroid use, diabetes, and underlying malignancy), which may overlap significantly with immunocompromised-related risk factors for SPE. Pre-existing pulmonary disease is also a risk factor for CNA [19].

Pulmonary tuberculosis:

Post-primary tuberculosis findings classically occur in the apical and posterior segments of the upper lobes and superior segments of the lower lobes [24], unlike the lower-lobe predominant preference of SPE. Miliary tuberculosis nodules present in random distribution, can also cavitate and present a feeding vessel sign, but are much smaller in size and range from 0.1 to 0.3cm [24], whereas nodule size is typically >0.5 cm in SPE. Calcified granulomas are another feature of tuberculosis absent in SPE [20]. Cavitory lesions, consolidation, centrilobular nodules and tree-in-bud pattern, macronodules, and galaxy sign also features of post-primary tuberculosis [20], the latter three of which are not apparent in SPE.

In summary, we report the first case of *S. mutans* native PVE complicated with SPE and a large pulmonary artery septic embolus. The diagnosis of SPE from right-sided endocarditis should be considered in patients with ancillary radiological findings of septic embolic phenomenon, particularly the presence of multifocal lower-lung predominant cavitory nodules and in the setting of appropriate predisposing factors such as pulmonic valve stenosis.

TEACHING POINT

Pulmonary valve endocarditis with a resultant large septic embolus of the main pulmonary artery is a rare finding, often requiring a high index of suspicion to secure the proper radiological diagnosis for an underlying infectious pathoetiology. The presence of coexisting peripheral, lower lobe-predominant, randomly distributed cavitory nodules and consolidations should prompt the radiologist to strongly consider a source of hematogenous source of infection, including right sided endocarditis.

REFERENCES

1. Park H, Cho G-Y, Kim H-K, Kim Y-J, Sohn D-W. Pulmonary Valve Endocarditis with Septic Pulmonary Thromboembolism in a Patient with Ventricular Septal Defect. *Journal of Cardiovascular Ultrasound*. 2009 Dec; 17(4):138. PMID: 20661339.
2. Sakuma M, Sugimura K, Nakamura M, et al. Unusual pulmonary embolism: septic pulmonary embolism and amniotic fluid embolism. *Circulation journal: official journal of the Japanese Circulation Society*. 2007 May; 71(5):772-5. PMID: 17457007.
3. MacMillan JC, Milstein SH, Samson PC. Clinical spectrum of septic pulmonary embolism and infarction. *J Thorac Cardiovasc Surg*. 1978; 75:670-679. PMID: 642559.
4. Song XY, Li S, Cao J, Xu K, Huang H, Xu ZJ. Cardiac septic pulmonary embolism. *Medicine*. 2016 Feb; 95(25). PMID: 27336870.
5. Goswami U, Brenes JA, Punjabi GV, Leclair MM, Williams DN. Associations and Outcomes of Septic Pulmonary Embolism. *The Open Respiratory Medicine Journal*. 2014; 8(1):28-33. PMID: 25184008.
6. Abdelbar A, Azzam R, Yap KH, Abousteit A. Isolated Pulmonary Infective Endocarditis with Septic Pulmonary Embolism Complicating a Right Ventricular Outflow Tract Obstruction: Scarce and Devious Presentation. *Case Reports in Surgery*. 2013 Aug; 2013:1-3. PMID: 24106634.
7. López-Pardo F, Aguilera A, Villa M, Granado C, Campos A, Cisneros JM. Double-Chambered Right Ventricle Associated with Mural and Pulmonic Valve Endocarditis: Description of a Clinical Case and Review of the Literature. *Echocardiography*. 2004 Feb; 21(2):171-3. PMID: 14961798.
8. Passen E, Feng Z. Cardiopulmonary manifestations of isolated pulmonary valve infective endocarditis demonstrated with cardiac CT. *Journal of Cardiovascular Computed Tomography*. 2015 Mar; 9(5):399-405. PMID: 25977113.
9. Ye R, Zhao L, Wang C, Wu X, Yan H. Clinical characteristics of septic pulmonary embolism in adults: A systematic review. *Respiratory Medicine*. 2014 Oct; 108(1):1-8. PMID: 24183289.
10. Fowler F, Scheld M, Bayer A. Endocarditis and Intravascular Infections. In: Bennett JE, Dolin R, Blaser MJ, Mandell GL, Douglas RG, eds. *Mandell, Douglas, and Bennett's Principles and practice of infectious diseases*. 8th ed. Philadelphia: Saunders Elsevier; 2015. p. 1004. ISBN: 978-1-4557-4801-3.
11. Cook RJ, Ashton RW, Aughenbaugh GL, Ryu JH. Septic Pulmonary Embolism: Presenting Features and Clinical Course of 14 Patients. *Chest*. 2005 Dec; 128(1):162-6. PMID: 16002930.
12. Huang R, Naidich D, Lubat E, Schinella R, Garay S, Mccauley D. Septic pulmonary emboli: CT-radiographic correlation. *American Journal of Roentgenology*. 1989 Jul; 153(1):41-5. PMID: 2735296.
13. Kwon WJ, Jeong YJ, Kim K-I, et al. Computed Tomographic Features of Pulmonary Septic Emboli: Comparison of Causative Organisms. *Journal of Computer Assisted Tomography*. 2007; 31(3):390-4. PMID: 17538285.
14. Kuhlman JE, Fishman EK, Teigen C. Pulmonary septic emboli: diagnosis with CT. *Radiology*. 1990. Jan; 174(1):211-3. PMID: 2294550.
15. Ricci KB, Lee PHU, Essandoh M, Kilic A. Fungal Pulmonary Valve Endocarditis Masquerading as a Pulmonary Embolism. *Case Reports in Surgery*. 2015 Jan; 2015:1-2. PMID: 25785222.
16. King PT. The pathophysiology of bronchiectasis. *International Journal of Chronic Obstructive Pulmonary Disease*. Nov 2009; 4:411-419. PMID: 20037680.

17. Raparla S, Schmidt EP, Pearse DB. Idiopathic constrictive bronchiolitis with rapidly progressive bronchiectasis and *Mycobacterium kansasii* infection. *Respiratory Medicine CME*. 2011;4(4):172-174. ISSN: 1755-0017.

18. Habib G, Lancellotti P, Antunes MJ, et al. 2015 ESC Guidelines for the Management of Infective Endocarditis. *Eur Heart J* 2015; Aug 29. PMID: 26320109.

19. Parkar AP, Kandiah P. Differential Diagnosis of Cavitory Lung Lesions. *Journal of the Belgian Society of Radiology*. 2016; 100(1):100. DOI: <http://doi.org/10.5334/jbr-btr.1202>.

20. Weerakkody Y, Vannod-Michel Q, Bridoux A, et al. Cavitating lung disease - a CT pictorial essay. Poster presented at The European Congress of Radiology 2014, 2014 March 6-10; Vienna, Austria.

21. Wittram C, Maher MM, Yoo AJ, Kalra MK, Shepard J-AO, Mcloud TC. CT Angiography of Pulmonary Embolism: Diagnostic Criteria and Causes of Misdiagnosis. *RadioGraphics*. 2004; 24(5):1219-38. PMID: 15371604.

22. Seo JB, Im J-G, Goo JM, Chung MJ, Kim M-Y. Atypical Pulmonary Metastases: Spectrum of Radiologic Findings. *RadioGraphics*. 2001; 21(2):403-17. PMID: 11259704.

23. Gadkowski LB, Stout JE. Cavitory Pulmonary Disease. *Clinical Microbiology Reviews*. 2008; 21(2):305-333. PMID: 18400799.

24. Nachiappan AC, Rahbar K, Shi X, et al. Pulmonary Tuberculosis: Role of Radiology in Diagnosis and Management. *RadioGraphics*. 2017 Jan-Feb;37(1):52-72. PMID: 28076011.

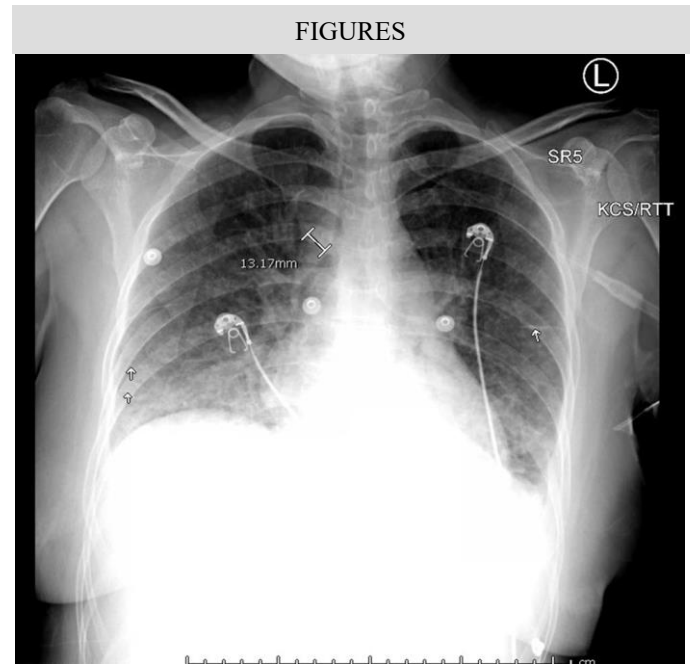


Figure 1: 41-year-old-female with septic pulmonary emboli secondary to pulmonary valve endocarditis. **FINDINGS:** Anterior-posterior portable chest radiograph demonstrates a prominent shadow of the azygos arch, widened vascular pedicle, and bilateral linear opacities with Kerley B lines (white arrows), suggestive of interstitial pulmonary edema. **TECHNIQUE:** Antero-posterior portable chest radiograph, 3 mA, 85 kVp.

www.RadiologyCases.com

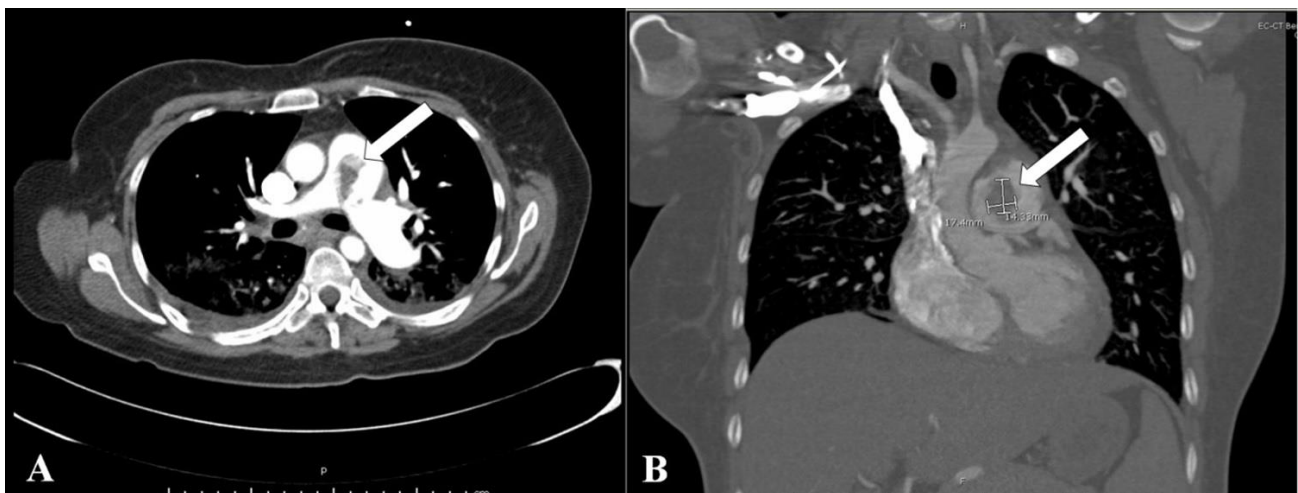


Figure 2: 41-year-old-female with septic pulmonary emboli secondary to pulmonary valve endocarditis. **FINDINGS:** (A) Axial image of the CT pulmonary angiography on soft tissue window at the level of the main pulmonary artery demonstrates a large filling defect at the bifurcation, consistent with a pulmonary embolus. (B) Coronal-reformatted image of the CT pulmonary angiography on bone window at the level of the main pulmonary artery just proximal to the bifurcation similarly demonstrates the large filling defect. No filling defects were seen distally in the remaining pulmonary arteries to the segmental level (not shown). No radiological evidence of heart strain was identified (not shown). **TECHNIQUE:** Axial computed tomographic pulmonary angiography (CTPA) with soft tissue windows (center: 55 HU, width: 426 HU) and coronal reconstructions with bone windows (center: 271 HU, width: 1718 HU), 479 mAs, 120 kV, 1.5 mm axial slice thickness, 3 mm slice coronal reconstruction, 100 ml Omnipaque 350.

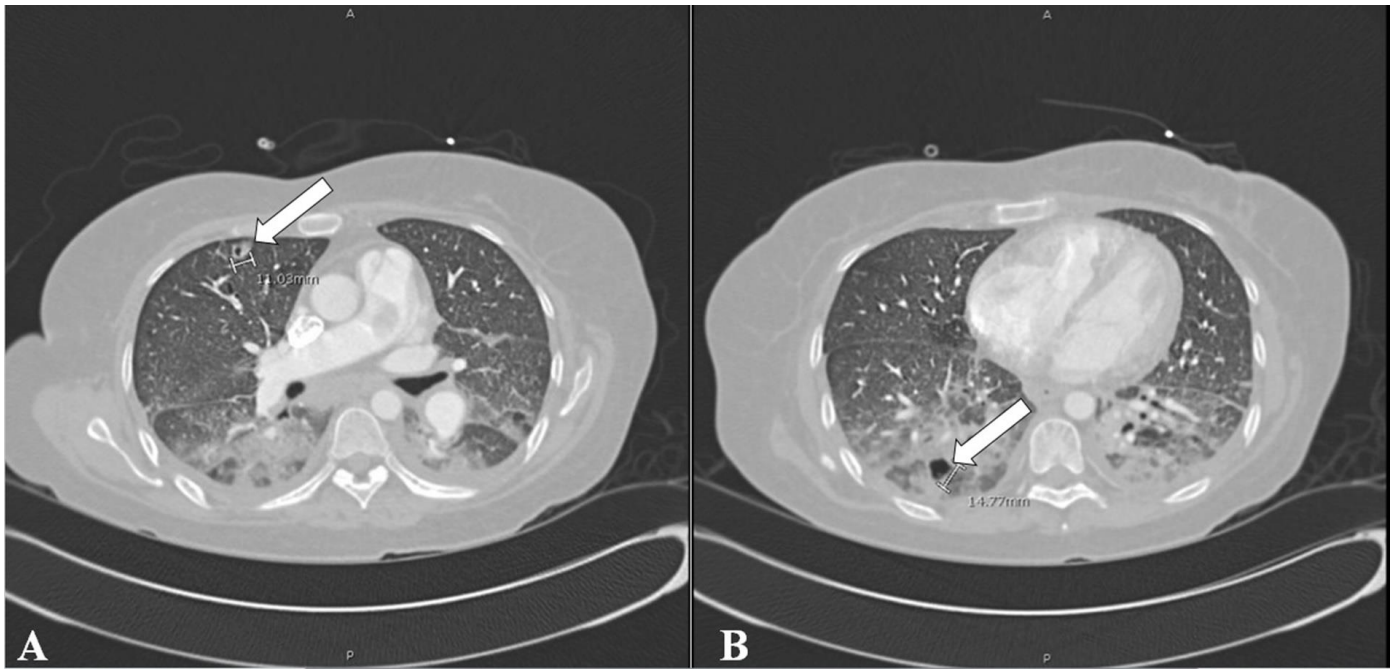


Figure 3: 41-year-old-female with septic pulmonary emboli secondary to pulmonary valve endocarditis.
FINDINGS: Axial views of CTPA on lung window at the level of the right main pulmonary artery (A) and at the 7th thoracic vertebra (B) demonstrate a peripheral cavitory nodule in the right upper and lower lobe, respectively. Four additional randomly distributed peripherally-located solid nodules up to 1.5 cm in size, some which were cavitory, were also present (not shown). Smooth interlobular septal thickening, lower lobe-predominant peribronchovascular thickening and consolidation, and patchy ground-glass opacities are also seen in both images, and are consistent with interstitial and alveolar pulmonary edema.
TECHNIQUE: Axial CTPA with lung windows (center: -400 HU, width: 2000 HU), 469 mAs, 120 kV, 1.5 mm slice thickness, 100 ml Omnipaque 350.

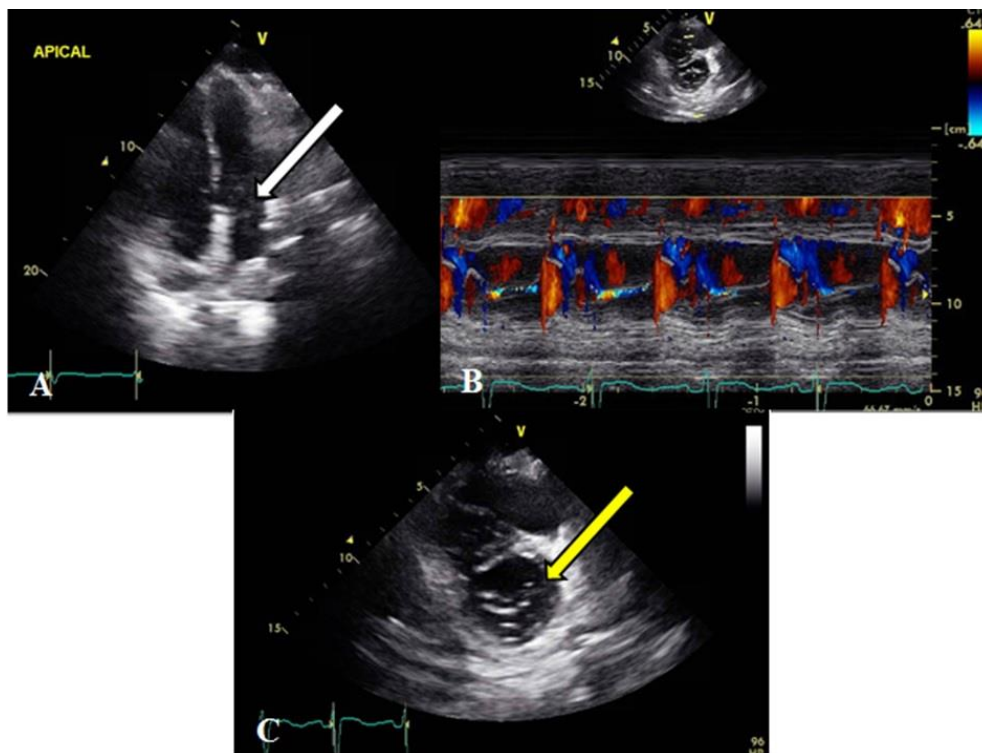


Figure 4: 41-year-old-female with septic pulmonary emboli secondary to pulmonary valve endocarditis.
FINDINGS: Transthoracic echocardiogram gray-scale views show a normal tricuspid valve (white arrows) on the apical four chamber view (A), with no vegetations. A flattened septum consistent with right ventricle pressure overload was noted, along with severe right ventricular dilatation. Doppler imaging of the pulmonary valve (B) revealed severe pulmonary stenosis with a peak pressure gradient of 80mmHg. A mildly mobile teardrop shaped thrombus in the proximal pulmonary artery (yellow arrow) was also visualized on a short axis view of the PA (C), corresponding with the filling defect found on CTAP.
TECHNIQUE: Transthoracic two-dimensional echocardiogram.

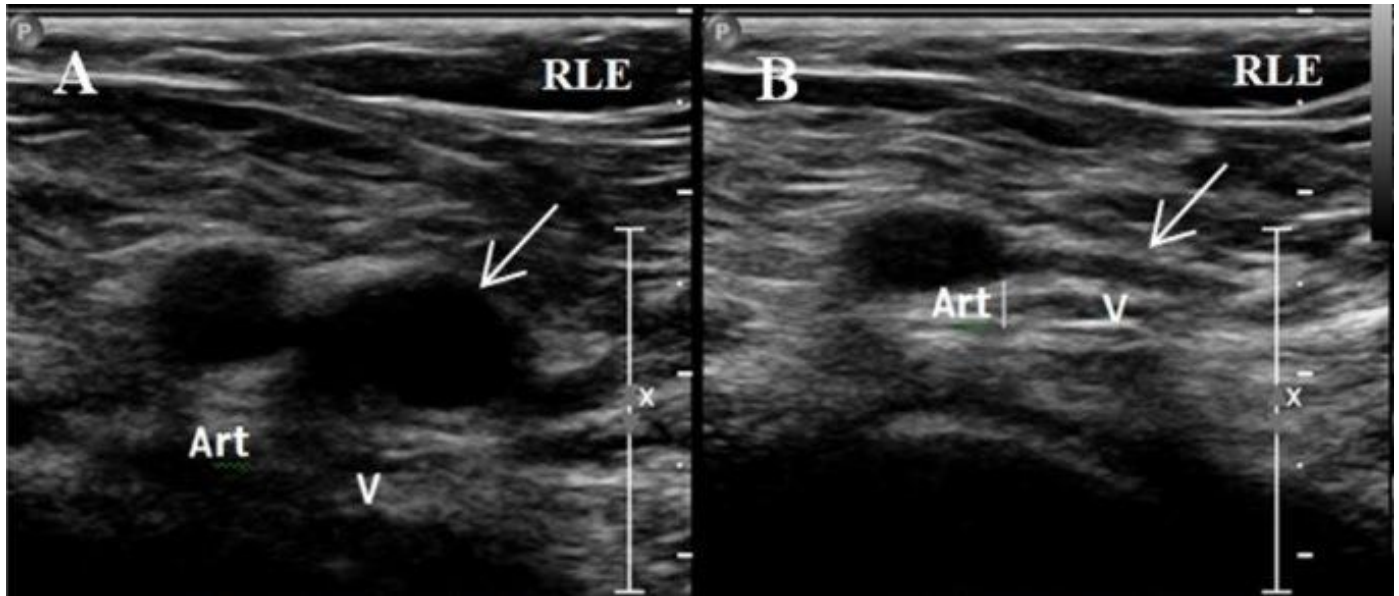


Figure 5: 41-year-old-female with septic pulmonary emboli secondary to pulmonary valve endocarditis.

FINDINGS: Transverse gray-scale ultrasound views of the common femoral vein (CFV) at the level of the saphenofemoral junction in the right lower extremity (A) demonstrate complete collapse of the veins (white arrows) when compression is applied with the transducer (B). Complete compression of the contralateral CFV and remaining upstream veins bilaterally was also noted. (Images not shown). Abbreviations: Art = common femoral artery, V = common femoral vein, RLE = right lower extremity.

TECHNIQUE: Linear transducer, 9-3MHz, gray-scale images.

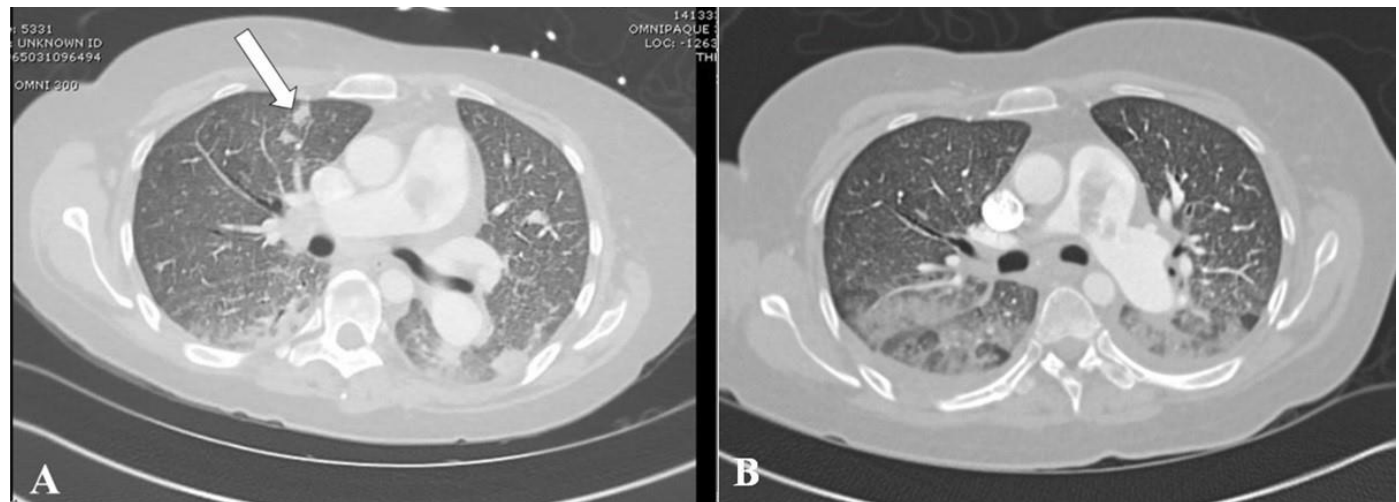


Figure 6: 41-year-old-female with septic pulmonary emboli secondary to pulmonary valve endocarditis.

FINDINGS: Axial views of a repeat CTPA on lung window at the level of the right main pulmonary demonstrate new peripheral solid nodules (white arrow) (A) when compared to the initial scan (B) at a similar level. The embolus at the bifurcation remained grossly stable.

TECHNIQUE: (A) Axial CTPA with lung windows (center: -600 HU, width: 2000 HU) 536 mAs, 100 kV, 2 mm slice thickness, 150 ml Omnipaque 300. (B) Axial CTPA with lung windows (center: -400 HU, width: 2000 HU), 469 mAs, 120 kV, 2 mm slice thickness, 100 ml Omnipaque 350.

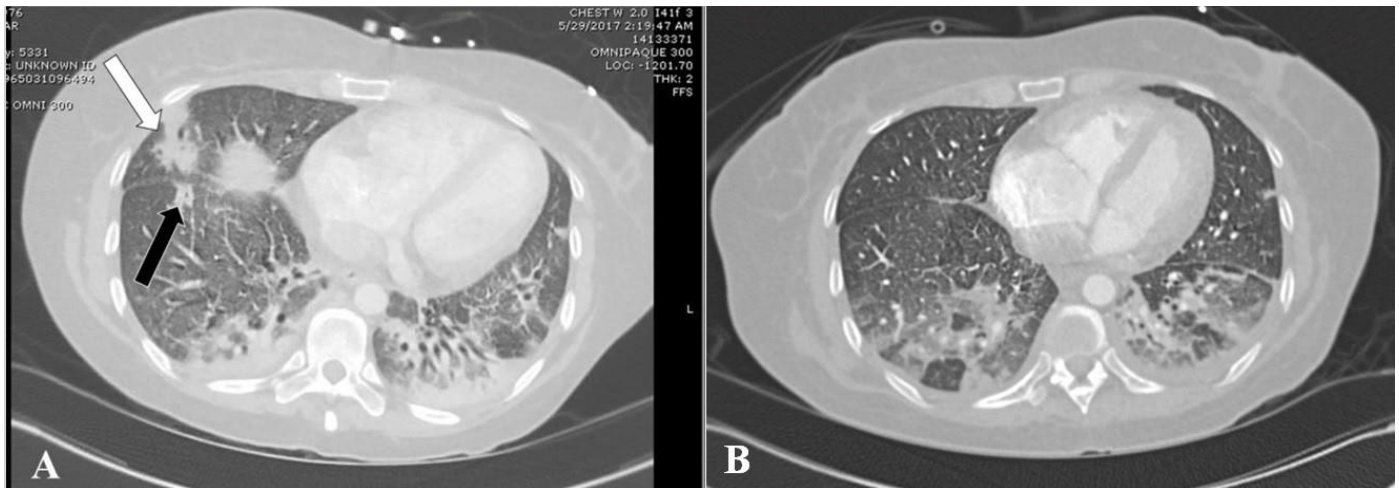


Figure 7: 41-year-old-female with septic pulmonary emboli secondary to pulmonary valve endocarditis.

FINDINGS: Axial view of the repeat CTPA on lung window more caudally at the level of the lower lobe segmental bronchi (A) demonstrates a new pleural-based consolidation in the lateral segment of the right middle lobe (white arrow) and a new cavitory nodule (black arrow) in the anterior segment of the right lower lobe, when compared to the initial scan (B). The degree of bilateral dependent consolidations has increased along with development of mild cylindrical bronchiectasis/bronchiolectasis, most notably seen in the left lower lobe.

TECHNIQUE: (A) Axial CTPA with lung windows (center: -600 HU, width: 2000 HU), 536 mAs, 100 kV, 2 mm slice thickness, 150 ml Omnipaque 300. (B) Axial CTPA with lung windows (center: -400 HU, width: 2000 HU), 347 mAs, 120 kV, 2 mm slice thickness, 100 ml Omnipaque 350.

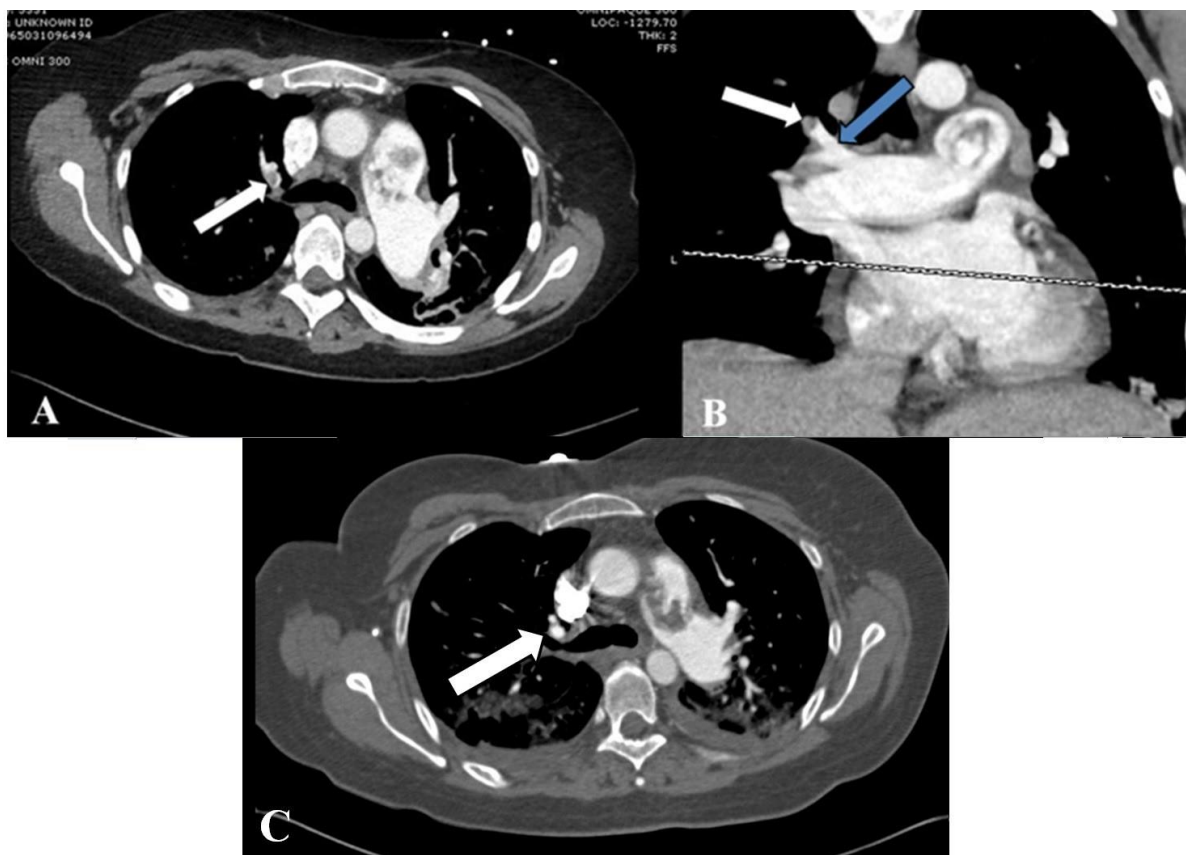


Figure 8: 41-year-old-female with septic pulmonary emboli secondary to pulmonary valve endocarditis.

FINDINGS: Axial and coronal views of the repeat CTPA on soft-tissue window at the level of carina (A, B) demonstrate a new filling defect in a right upper lobe segmental pulmonary artery (white arrow) when compared to initial scan at a similar level (C). The origin of the occluded vessel can be seen extending from the truncus anterior (blue arrow) on the coronal view (B). The large embolus in the main pulmonary artery remains grossly unchanged.

TECHNIQUE: (A, B) Axial and coronal CTPA with soft tissue window (center: 50 HU, width 400 HU), 536 mAs, 100 kV, 2 mm axial slice thickness, 3 mm coronal reconstruction, 150 ml Omnipaque 300. (C) Axial CTPA with soft tissue window (center: 100 HU, width: 800 HU), 416 mAs, 120 kV, 1.5 mm slice thickness, 100 ml Omnipaque 350.

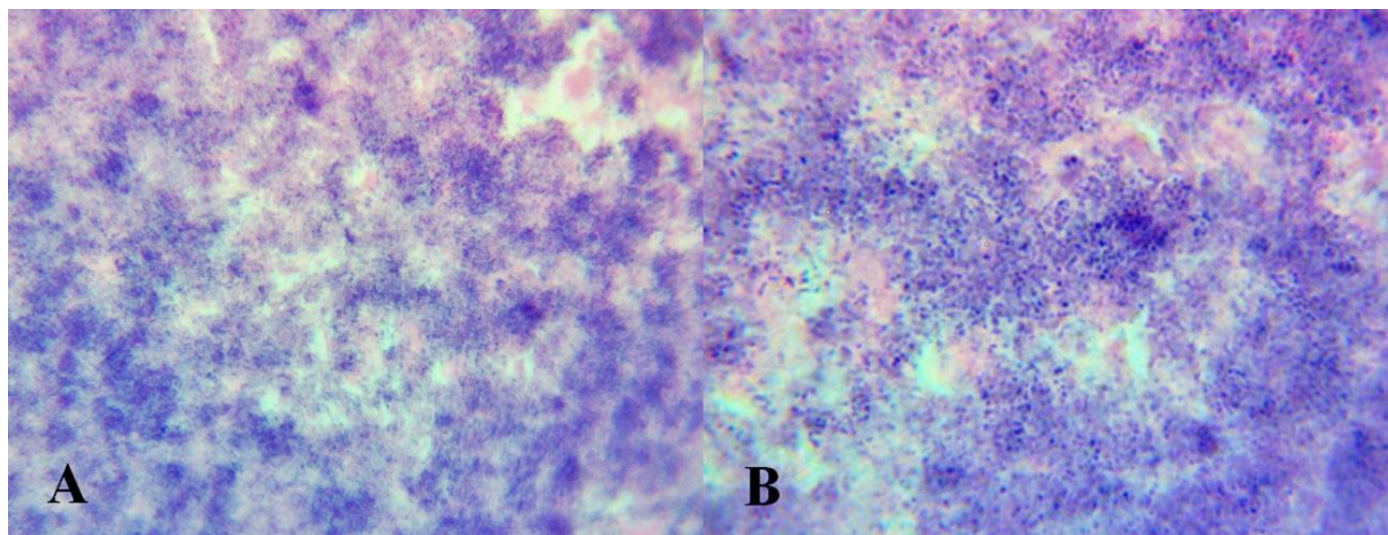


Figure 9: 41-year-old-female with septic pulmonary emboli secondary to pulmonary valve endocarditis.

FINDINGS: Histological examination with hematoxylin and eosin staining of the pulmonary artery thrombus revealed abundant bacteria in a fibrin thrombus.

TECHNIQUE: Hematoxylin and eosin staining, 40x magnification (A) and 100x magnification (B). Courtesy of Ashley Holloman, M.D.

Etiology	Extrapulmonary infections: Right-sided infective endocarditis, infected central lines or devices, deep soft tissue infections, septic thrombophlebitis (e.g. internal jugular and pelvic veins), abscesses.
Microbiology	<i>Staphylococcus aureus</i> is the most common agent. Methicillin resistant <i>S. aureus</i> represents 40% of all <i>S. aureus</i> cases. Other common agents: <i>Candida sp.</i> , <i>Fusobacterium sp.</i> , <i>Klebsiella pneumoniae</i> and <i>Streptococcus viridans</i> .
Prevalence	2.2% of all pulmonary embolism cases.
Gender ratio	Males = Females.
Age predilection	None.
Risk factors	Intravenous drug use, right-sided prosthetic valves, indwelling catheters and devices, alcoholism, immunodeficiency (solid and hematological cancers, diabetes mellitus, organ transplantation).
Treatment	Antibiotics and source control of the underlying extrapulmonary infection. Surgical management may be indicated for source control. (e.g. valve replacement). Anticoagulation is controversial and may be contraindicated in individual cases.
Prognosis	Mortality ranges from 10 - 20% despite treatment. Most commonly due to septic shock and multi-organ failure.
Findings on imaging	Chest radiography: commonly nonspecific lower lobe airspace opacities and pleural effusions. Chest CT: Bilateral, multiple, lower lobe-predominant, peripheral soft tissue density nodules is the most common finding. Cavitation, feeding vessel sign, CT halo sign, wedge-shaped pleural-based consolidations, and pleural effusions may occur. CTPA: 50% with filling defects in segmental/subsegmental pulmonary arteries. Large central filling defects are rare.

Table 1: Summary table for septic pulmonary emboli.

	Chest CT features	CTPA features
Septic pulmonary emboli	-Bilateral, lower lobe-predominant, peripheral pulmonary nodules with cavitation. -Multiple (>10) nodules occur in 1/3. -Nodules size ranges from 0.5 – 3.5 cm. -Feeding vessel sign, CT halo sign and wedge-shaped pleural-based consolidation. -Nodules cavitate and evolve over hours to days.	-Filling defects in segmental and subsegmental pulmonary arteries. Central filling defects are rare.
Metastatic cancer	-Multiple randomly distributed cavitory nodules, of varying sizes and wall thickness. -Nodules evolve over months	-Large filling defects possible with tumor emboli.
Granulomatosis with polyangiitis	-Large, 2-4cm, central cavitory nodules. -Number of lesions <10.	-No filling defects.
Necrobiotic lung nodules	-Bilateral, peripheral pulmonary nodules with cavitation.	-No filling defects.
Chronic necrotizing aspergillosis	-Frequently solitary slow-growing apical nodule. -Feeding vessel and CT halo signs possible.	-No filling defects.
Post-primary tuberculosis	-Upper lobe and superior segment of lower lobe predominance. -Centrilobular nodules and tree-in-bud pattern, galaxy sign, macronodules, and consolidation. -Random distribution and nodule size in miliary TB ranges from 0.1 – 0.3cm. -Calcified granulomas.	-No filling defects.
Bland pulmonary embolism	-Lack of cavitory nodules. -Pleural-based wedge-shaped consolidation and feeding vessel sign.	-Filling defects in both central and segmental pulmonary arteries.

Table 2: Differential diagnosis table for septic pulmonary emboli on chest CT and CTPA.

ABBREVIATIONS

- Art = common femoral artery
- CNA = chronic necrotizing aspergillosis
- CNS = central nervous system
- CT = computed tomography
- CTPA = computed tomographic pulmonary angiography.
- GWP = granulomatosis with polyangiitis
- NLN = necrobiotic lung nodules
- PVE = pulmonary valve endocarditis
- RLE = right lower extremity
- SPE = septic pulmonary emboli
- V = common femoral vein

KEYWORDS

Endocarditis; pulmonary valve; septic pulmonary embolism; septic pulmonary emboli; pulmonary artery; computed tomographic pulmonary angiography; computed tomography

ACKNOWLEDGEMENTS

The authors would like to thank Ashley Holloman M.D. for providing the histological images.

Online access

This publication is online available at:
www.radiologycases.com/index.php/radiologycases/article/view/3240

Peer discussion

Discuss this manuscript in our protected discussion forum at:
www.radiolopolis.com/forums/JRCR

Interactivity

This publication is available as an interactive article with scroll, window/level, magnify and more features.
Available online at www.RadiologyCases.com

Published by EduRad



www.EduRad.org